A detailed comparison of experimental and theoretical stress-analysis of a human femur

A DETAILED COMPARISON OF EXPERIMENTAL AND THEORETICAL STRESS-ANALYSES OF A HUMAN FEMUR

R. Huiskes*, J. D. Janssen and T. J. Slooff
Division of Applied Mechanics, Department of Mechanical Engineering
Eindhoven University of Technology, and the Department of Orthopaedics
University of Nijmegen, The Netherlands

*Presently on leave at the Biomechanics Laboratory, Department of Orthopedics
Mayo Clinic/Mayo Foundation
Rochester, Minnesota

ABSTRACT

Experimental strain-gauge and theoretical stress analysis methods are used to evaluate the mechanical behavior of the femur as a structural element under loading. It is shown that when the cortical bone material is assumed to behave linear elastic, homogeneous and transversely isotropic, excellent agreement between experimental results and theoretical predictions is obtained. Also that the bone shaft can with reasonable approximation be represented by an axisymmetric model, even when intramedullary hip joint prostheses are present. The implications of these results for the analysis of intramedullary bone-prosthesis structures are discussed.

INTRODUCTION

Stress analysis of long bones is by no means a new field; it is said that the earliest publication dates back to Galileo in 1638. Well-known contributions to an understanding of the mechanical behavior of the femur, the favorite bone of biomechanicians, were published in the second half of the last and the first half of this century. An excellent review of this earlier work has been presented by Evans [1]. In recent years, many studies have been devoted to the mechanical properties of bone and the mechanical behavior of bones. Many of these were in some way connected to the analysis of bone-prosthesis structures for optimal joint prosthesis designs, as applied in orthopaedic surgery. In analyses of this kind, as in this paper, the bone is considered as a structural element, an entity of continuum materials, and the objective is to evaluate its stress and deformation patterns as functions of loading, geometrical and material parameters. It should be kept in mind that, within the scope of "Biomechanics of Bone," this approach differs from studies where bone is considered as a material, the bone-tissue composite, or as a structure. The latter structure is the continuum material of the structural element, while the bone-tissue composite is the continuum material of the bone structure. Hence, the difference lies in the level of model refinement, which depends on the objectives of the analysis. For instance, cortical bone is no doubt anisotropic and nonhomogeneous, which is of importance when the structure of this material is studied. However, in structural analyses of entire bones these refinements need to be taken into account only so far as they significantly affect their gross mechanical behavior. Exactly what "significantly" means in this case, quantitatively speaking, again

depends on the objectives of the analysis.

This paper principally addresses the problems of modelling long bones, mainly the diaphyses, in their geometrical and material aspects for structural stress analyses, intact as well as provided with prostheses. The objective is to investigate the possibilities and evaluate the accuracies of different models, using experimental as well as theoretical methods.

It is interesting to see how the development of stress analyses of the intact femur through the years follows the introduction and development of analysis methods in applied mechanics. Experimental stress-coating methods [e.g. 2,1,3], photoelastic model studies [e.g. 4,5], extensometers [e.g.6,3], and strain gauges [e.g. 1,7,8,9,10] have been used subsequently. Theoretical analyses have been reported using Culmann's trajectorial diagram [11], beam theory [e.g. 12,13,14,15], two-dimensional Finite Element Methods (FEM) [e.g. 16,14,17, 15], and three-dimensional FEM [e.g. 18,15,19,20]. Although these efforts have contributed tremendously to a better understanding of the femoral functional morphology, the occurrence of stress and deformation patterns under various loading cases, and the structural strength of the bone, few investigators have addressed questions of modelling accuracy. Exceptions are the studies of Scholten [15], who compared results of 2-D, 3-D FEM studies and beam analysis in detail, finding that a good agreement of results can be obtained in the femoral shaft, up to the subtrochanteric region, and Valliappan et al. [19], who roughly compared results of 2-D FEM analyses, beam analysis and experimental stress-coat analyses, finding good agreement in a relative sense. However, the only precise and well-defined comparison between theoretical and accurate experimental results of which this author is aware, was published by Rohlmann et al. [10]. They analyzed a cadaveric femur under loading, using both strain gauges and FEM to determine the stresses. They found reasonable relative but poor absolute agreement between results of both methods. They concluded that the discrepancies were caused by slight geometrical inaccuracies of the FE model, the rough approximation of the bone properties in the model, and the roughness of the FE mesh.

It is shown here that theoretical models using FEM should be able to accurately represent at least the diaphysis of the femur with respect to its gross mechanical behavior as a structural element, provided that the anisotropic properties of the cortical bone are recognized. These properties can be adequately described using the transversely isotropic theory as proposed by Carter [21], based on data from Reilly and Burstein [22]. For a number of applications, however, the bone material can be assumed to be isotropic, and linear three-dimensional beam theory can be applied with quite acceptable accuracy. It is also shown that the bone shaft can be approximated reasonably well with an axisymmetric geometry. The implications of these findings for stress analyses of intramedullary bone-prosthesis structures are discussed.

METHODS

Both femurs of a 52 year-old male were used for the analyses. The left femur, embalmed with formaline, was fixed in a laboratory setting and applied with 100 strain-gauge rosettes, 3 elements each in a rectangular configuration, on the femoral shaft (Fig. 1). The strain rosettes (type PR-5-11, Tokyo Sikk Kenyojo, Ltd.), with diameters of 5 mm approximately, were glued with 2-component Schnellklebstof X60 (Hottinger Baldwin Messtechnik G.M.B.H.) after local drying of the bone surface. The distal side of the bone was fixed in a steel box, while the femoral head was provided with a brass cap for the application of loads. After gluing of the gauges, their center point positions in space were measured with an accuracy of 0.1 mm.

Twelve different loads were applied in turn to the femoral head (Fig. 2): forces in three directions, positive and negative, and couples in three planes, positive and negative. Loads were applied from zero to full load in one second approximately. Strain measurement was started three minutes after application of the load in order to allow for viscous effects to diminish. For each loading

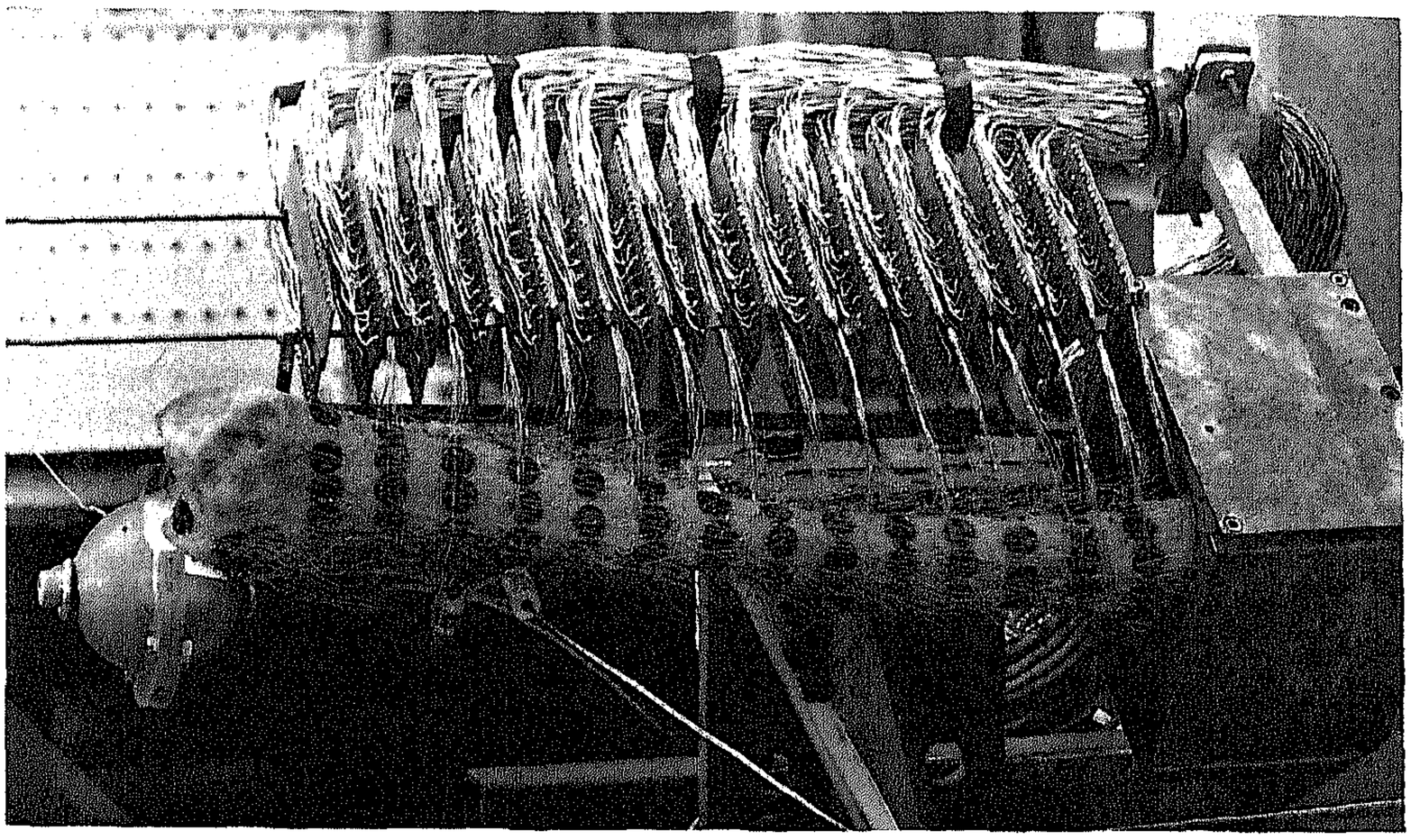

Fig. 1 The experimental femur with strain-gauge rosettes.

case, the element strains were recorded using an automatic strain-gauge measuring system (2 pnts/sec) and punched on tape. A low excitation voltage was used (1.25V) to limit effects of local bone heating. A dummy strain gauge attached to an unloaded bone piece compensated for temperature and humidity effects.

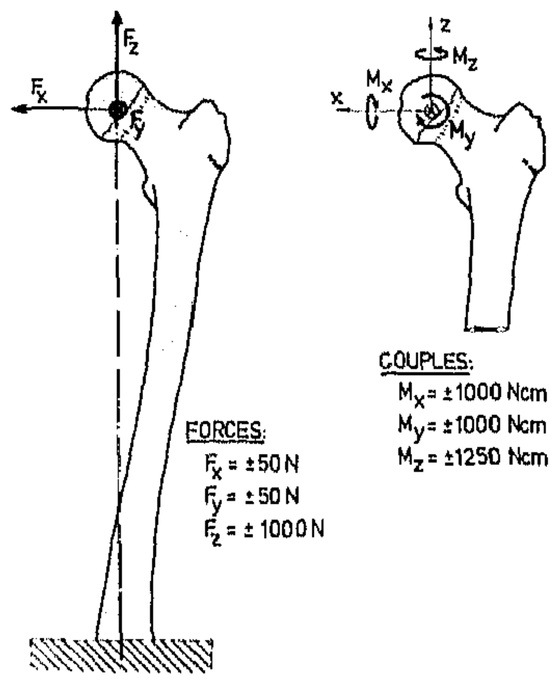

Fig. 2 Loads applied in turn on the femoral head.

After analysis of the intact bone, the same femur was provided in turn with various implants (Küntscher nails of various dimensions; long and short Moore hip prostheses, not cemented; long and short Müller hip prostheses, cemented; and bone-fracture plates) and the measurements were repeated. Not all these cases are discussed here, however.

The measured strains were processed by computer to calculate principal strains (ε_I, ε_{II}) and principal strain orientations (ϕ) with respect to the longitudinal bone axis. Stresses were calculated from strains in two different ways:

- Isotropic Analysis: Assuming the bone Young's modulus to be 20,000 MPa and its Poisson's ratio 0.37, principal strains (ε_I, ε_{II}) were used to calculate principal stresses (σ_I, σ_{II}), applying Hooke's law for this case. Equivalent von Mises stresses were calculated from: $\sigma_{eq} = |\sigma_I - \sigma_{II}|$.

- Anisotropic Analysis: As proposed by Carter [21], based on data from Reilly and Burstein [22], the bone material was assumed to be transversely isotropic. Fig. 3 shows a local coordinate system for each strain gauge. The principal material directions are denoted by axis 1 (= z-axis, the longitudinal bone direction) and axis 2 (= s-axis, the tangential bone direction, related to the z-axis according to the left-hand rule). The principal strain directions are denoted by the axes I and II (orientation angle ϕ), and the principal stress direction by the axes A and B (orientation angle ξ).

  The strains in the material directions (ε_1, ε_2, γ_{12}) can then be calculated from ε_I, ε_{II} and ϕ [21], and the stresses in the material directions from:

$$\begin{bmatrix} \sigma_1 \\ \sigma_2 \\ \tau_{12} \end{bmatrix} = \begin{bmatrix} S_{11} & S_{12} & 0 \\ S_{12} & S_{22} & 0 \\ 0 & 0 & S_{33} \end{bmatrix} \begin{bmatrix} \varepsilon_1 \\ \varepsilon_2 \\ \gamma_{12} \end{bmatrix}$$

with $S_{11} = E_{11}/(1 - \nu_{12}\nu_{21})$, $S_{22} = E_{22}/(1 - \nu_{12}\nu_{21})$, $S_{12} = E_{11}\nu_{21}/(1 - \nu_{12}\nu_{21})$ and $S_{33} = G_{12}$, where E are Young's moduli, ν Poisson's ratios and G the shear modulus [21]. In accordance with [21] and [22], it was assumed that

$$E_{22} = 0.68\ E_{11},\ G_{12} = 0.19\ E_{11},\ \nu_{12} = 0.46 \text{ and } \nu_{21} = 0.31$$

Here, as in the isotropic analysis the longitudinal Young's Modulus was taken as E_{11} = 20,000 MPa. It follows that the transverse modulus E_{22} = 13,600 MPa, and the shear modulus G_{12} = 3,800 MPa (in the isotropic analysis $G = E/2(1 + \nu) \approx 7{,}299$ MPa).

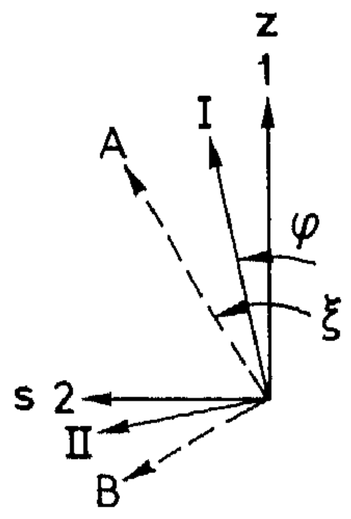

Fig. 3 Local coordinate system for each strain gauge. (1, 2 material axes, z = longitudinal bone direction, s = tangential bone direction; I, II principal strain axes; A, B principal stress axes).

The right femur of the same cadaver was imbedded in Araldite and sliced into thirty cross sections. Fig. 4 shows the positions of the sections C7 through C24, relative to the planes S_1 through S_{14} in which the strain gauges were glued on the other femur. The strain-gauge planes are not always identical with the sections, as shown in Fig. 4, which requires some interpolation in the comparisons, discussed later.

The bone contours in each section were digitized on an x-y coordinate measuring table. Cross-sectional areas (A, mm^2), maximal and minimal area moments of inertia (I_{max} and I_{min}, mm^4), polar moments of inertia (J, mm^4), positions of gravity centers, and inertia axis orientation (α) with respect to the section coordinate system (x', y') were calculated. An approximative axisymmetric cross section was calculated for each section as well (inner radius r (mm) and outer R (mm)) in such a way that both the area and the polar moment of inertia are represented exactly, according to

$$R^2 = \frac{J}{A} + \frac{A}{2\pi} \text{ and } r^2 = \frac{J}{A} - \frac{A}{2\pi}$$

It follows that the area moment of inertia of the axisymmetric cross section $I_{appr} = J/2$.

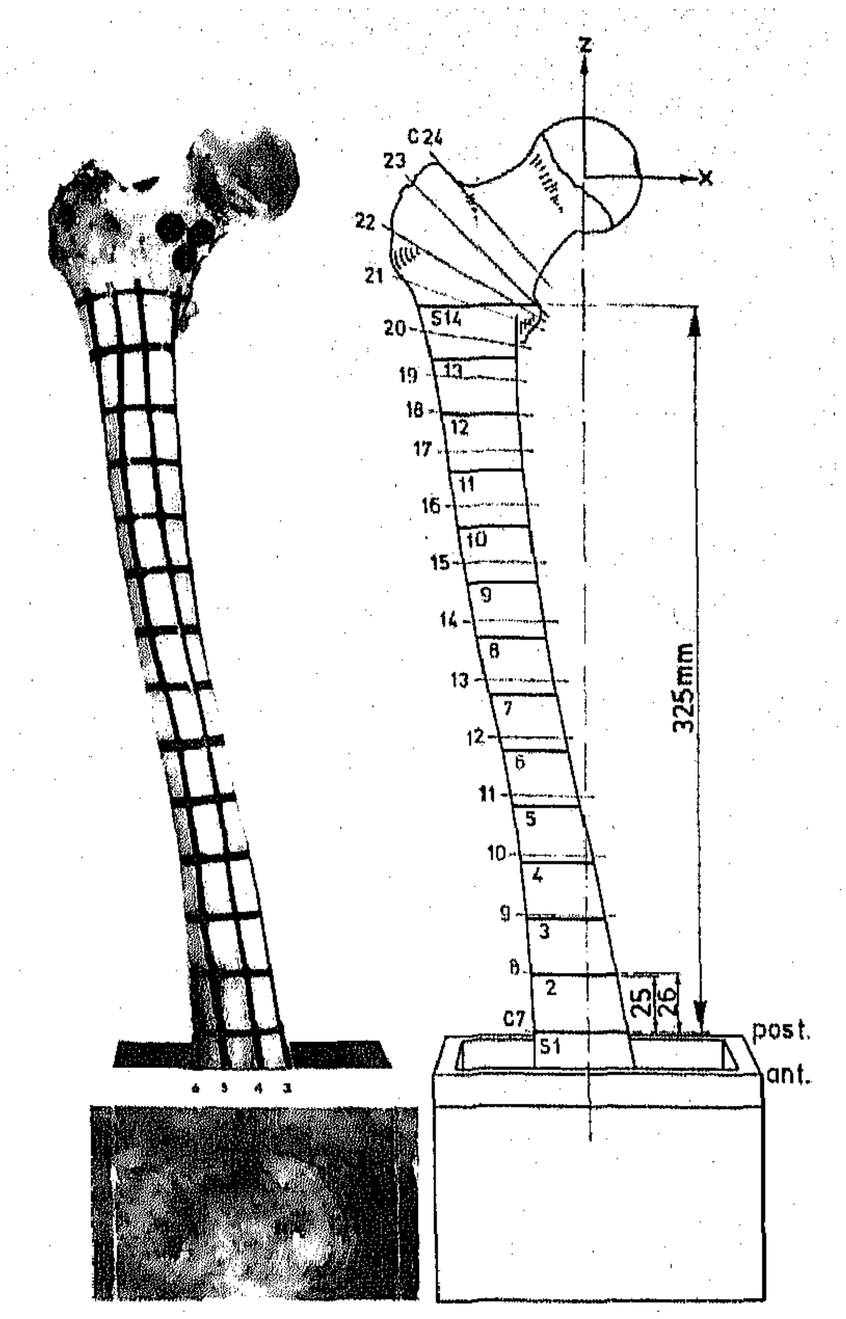

Fig. 4 Strain gauges were located on the crossings of the black lines (left). Sections (C) and strain-gauge levels (S) are shown right.

Axial direct stresses at a number of points in each cross section were calculated for all loading cases except torsion by applying three-dimensional beam theory (uniaxial stress state). These stresses are in the longitudinal material direction.

Shear stresses in the cross sections upon torsional loading of the bone were calculated in two ways:

- Using the axisymmetric geometry for each section, the maximal shear stresses at the bone surfaces (τ_m) were approximated by

$$\tau_m = \frac{M_z R}{J}$$

For one cross section (C12), the shear stresses due to torsion were calculated using the theory of Saint Venant [23]. The resulting elliptical differential equation describing the stress-function in the cross section, and the boundary conditions were solved using a Finite Element program for this purpose [24]. The section was divided into 792 triangular elements with three nodal points each. Maximal shear stresses were calculated at the centers of gravity of each element. It should be mentioned that this method has been used previously for bone cross sections [25,26,27].

RESULTS

The strain gauge measurements on the femur, both intact and with implants, were carried out between October, 1971 and July, 1974. Seven of the one hundred rosettes failed in the course of time. The other ninety-three showed no significant deviations in values when control measurements were carried out at three different times during the two and one-half year period.

The reproducibility of the measured strain values, evaluated by loading the bone seven times with a force of 1,000 N in the negative z-direction, was better than 1%. Fig. 5 shows the spread in equivalent stress and principal strain orientation values, as calculated from strains obtained in this test for a longitudinal row of strain gauges.

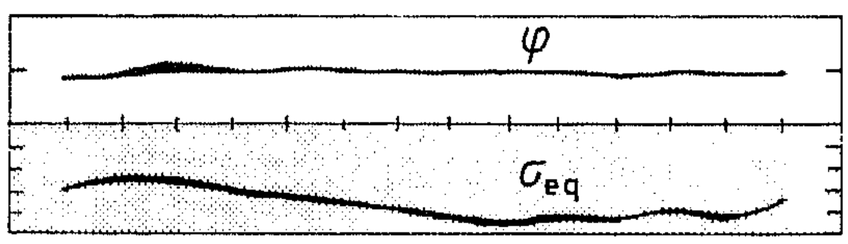

Fig. 5 Spread of equivalent stress and principal-strain orientation angles found from 7 subsequent tests with a 1,000 N force in negative z-direction, on a distal to proximal strain-gauge row.

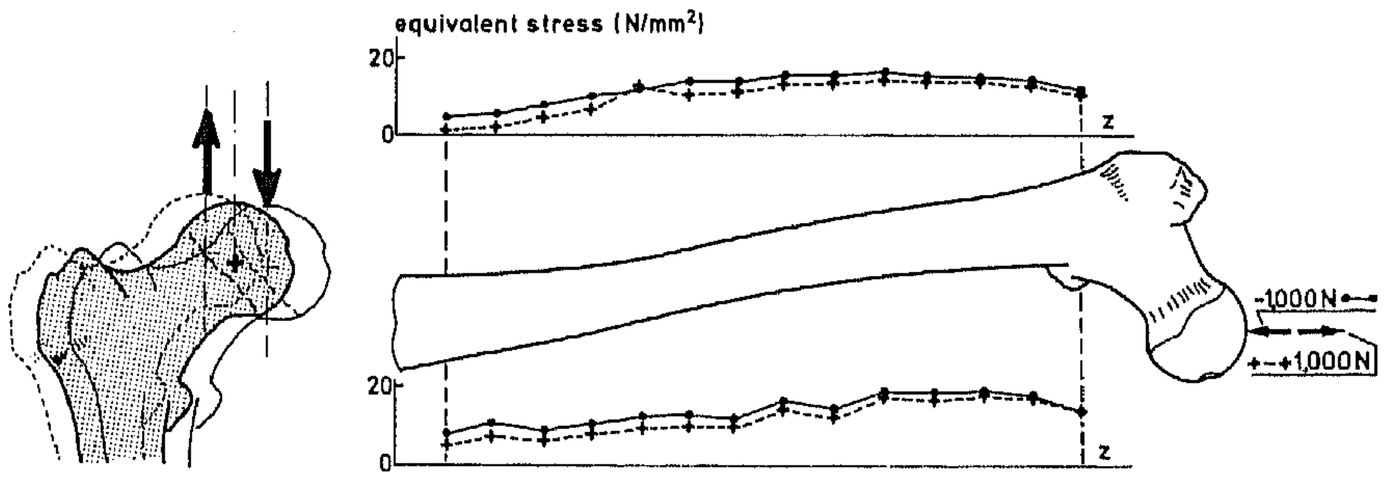

Fig. 6 Positive and negative forces on the head do not result in equal stress (and strain) values in the absolute sense, due to geometrically nonlinear effects caused by transverse displacements of the head (left). Here comparisons of equivalent stresses are shown (right), on a medial and a lateral strain-gauge row.

In another test it was found that for loads as applied here, the strain values did not change significantly in a period from three minutes to seventy-two hours after load application. For that reason, recording of strains started only three minutes after load application in each experiment.

By comparing the resulting strains for positive and negative couples, it followed that the bone material behaved in a linear elastic manner, at least for the loads as applied here. Differences were less than 2%. Geometrically non-linear behavior, however, was evident from comparing the results of positive and negative forces (1,000 N) in the z-direction (Fig. 6). The differences in strain values are caused by the additional couples, introduced by head displacements in the transverse direction. This, of course, does not occur in loading with pure couples.

Cross-sectional Properties

The cross sections C5 through C21 are shown in Fig. 7 with their principal inertia axes, as determined from the digitized cross-sectional shapes. Other cross-sectional properties are shown in Fig. 8, including the radii (R and r) of the axisymmetric approximation. The cross-sectional area (A) appears to be fairly constant throughout the region considered. The moments of inertia (I_{max} and I_{min}) increase significantly at the proximal and distal sides. The principal axis orientation angle (α) is measured to either the maximum or minimum axis; hence, its high gradients near cross section C12 do not reflect its real behavior, which is rather smooth (see Fig. 7).

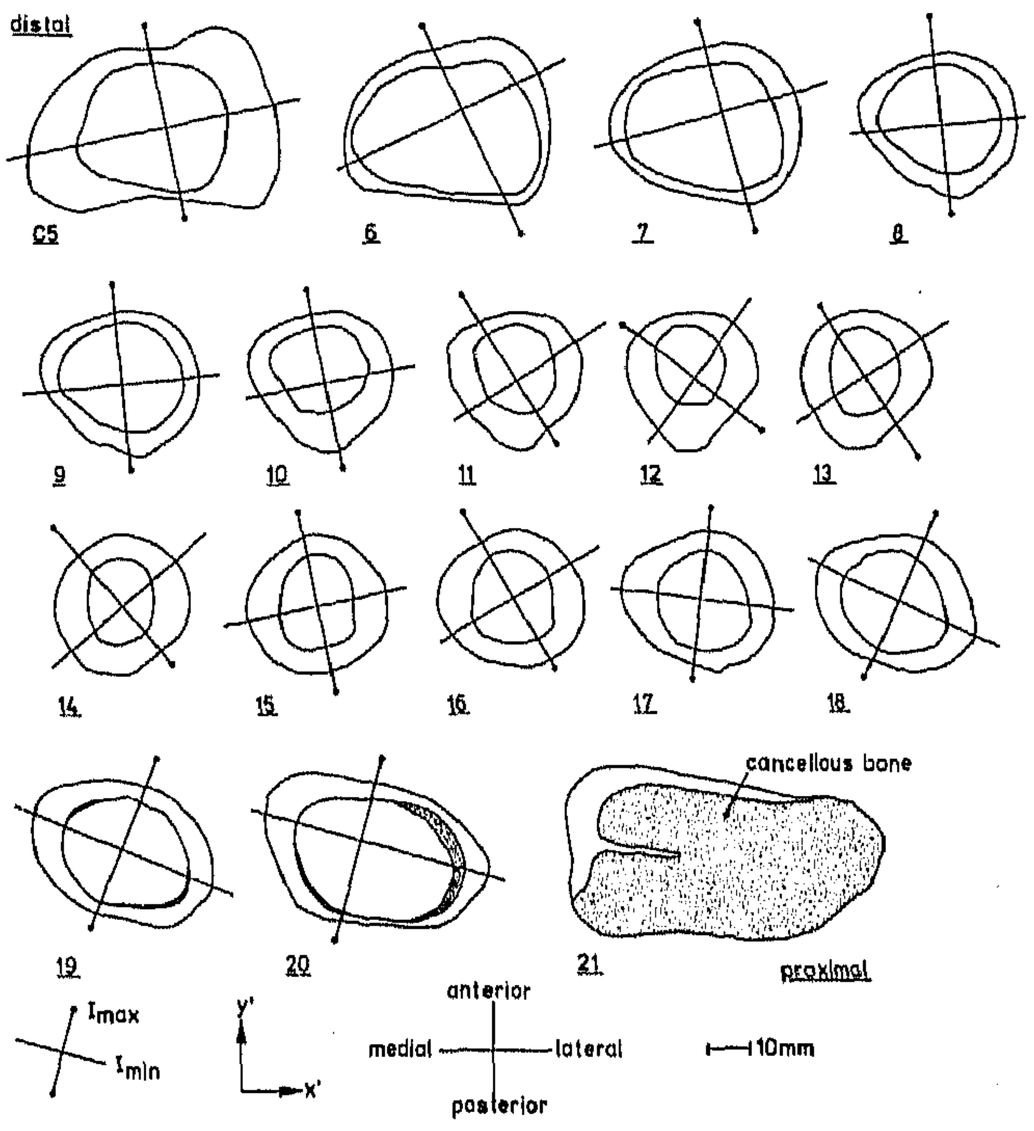

Fig. 7 Geometry and principal inertia axes of sections C5 through C21 (in section C5 cancellous bone is not shown).

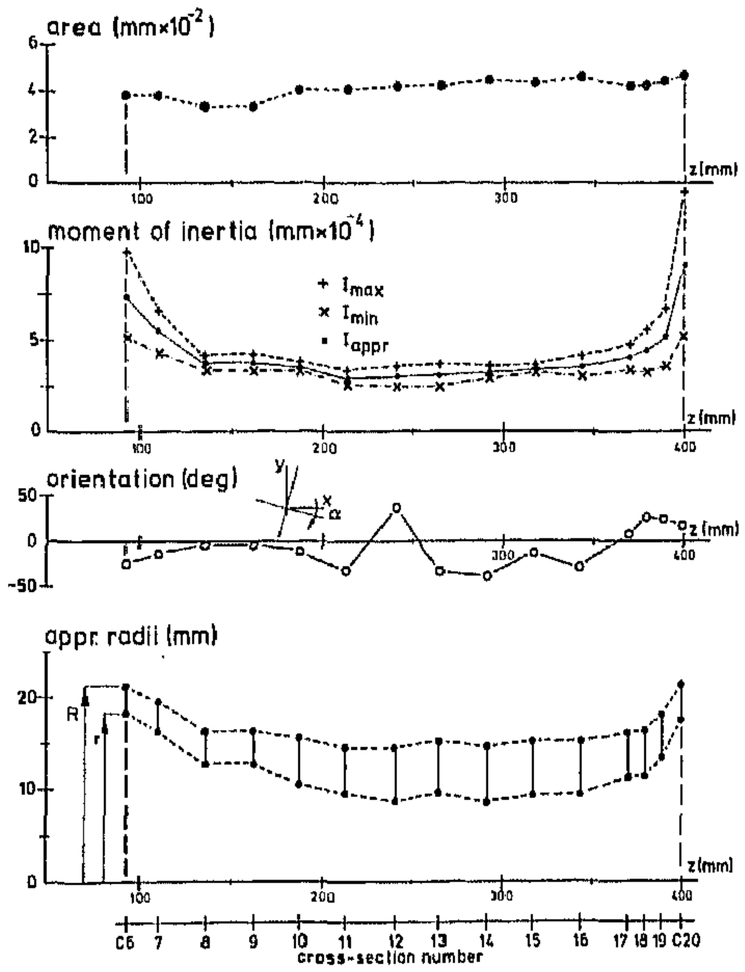

Fig. 8 Properties of the sections (A, I_{max}, I_{min}, α) and the axisymmetric approximations (I_{appr}, R, r).

Overall Comparison of Data

Figure 9 shows a comparison of principal stresses as evaluated from the experiment (isotropic analysis) and as calculated using 3-D linear beam theory, at various levels of the intact bone, for a force of 1,000 N in the negative z-direction. The levels a through f are equivalent to the sections C7, C9, C11, C13, C15 and C17; level g is equivalent with strain-gauge plane S14 (see Fig. 4). Where strain-gauge planes and section levels did not coincide, the experimental results were interpolated.

The agreement between both sets of results is reasonably good. The geometrically nonlinear behavior of the bone in the experiment would call for the stresses to be lower on the lateral and higher on the medial side, which is generally the case. In the beam analysis, the principal stress directions of course coincide with the section plane and the bone axis. In the experiments, this is not necessarily the case. Figure 10 shows principal strains as resulting from this experiment. The surface of the femur is represented in a flat plane and principal strain directions are shown with respect to the bone axis. Because the analysis is isotropic in this case, these directions are equal to the principal stress directions. The orientation is by no means always in the material direction, but for the most significant strains the deviations are slight. However, the discrepancies shown in Fig. 9 may partly be caused by these deviations. Other sources of discrepancies between measured and predicted stresses are thought to be local differences in geometries of the left and the right femur, the approximative character of the comparison (interpolation), local differences in bone stiffness, anisotropic behavior, and random measurement errors.

When results of pure couple loading are compared, as in Figs. 11 and 12, geometrical nonlinearity is not a source of discrepancies. Here, the agreement is indeed somewhat better, especially for the couple around the y-axis (Fig. 11), which is the more physiological kind of loading. When results of all three loading cases are considered (Figs. 9, 11 and 12), it is evident that the discrepancies in measured and predicted values are the highest in level f.

Hence, it is probable that here the interpolation procedure or differences in left and right bone geometries play a major role. Large discrepancies (50%) are apparent on level a, upon loading with a couple around the x-axis. Since strain-gauge plane and section are the same in this case, and agreement for M_y is good for this level, it is probable that here local differences in bone stiffness play a role.

Results from other loading cases (F_x and F_y) give comparable results, qualitatively speaking, to the ones discussed here. Also, comparisons of data on other levels as the ones shown here do not give additional information. Results of torsion are discussed later.

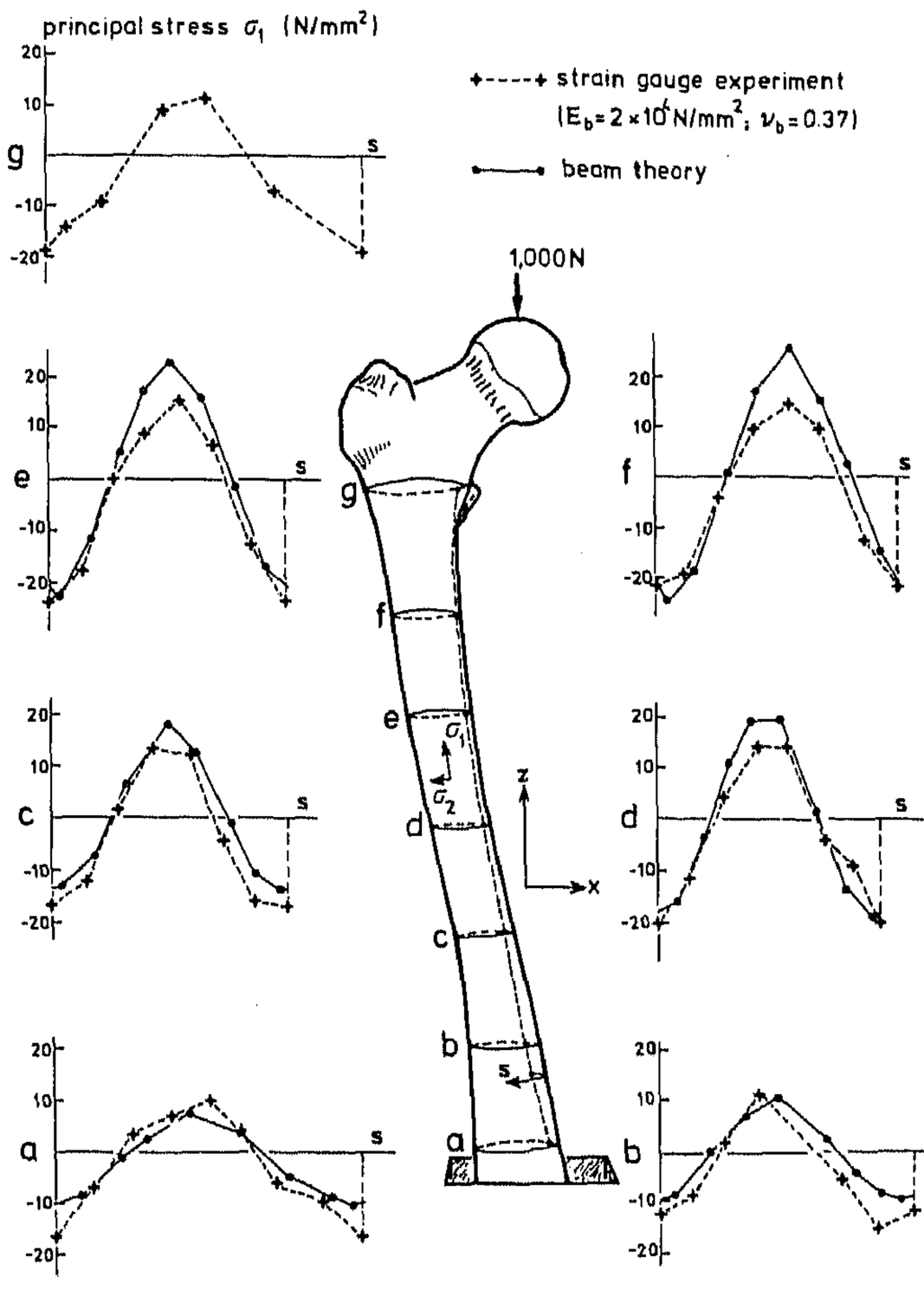

Fig. 9 Comparison of principal stresses as evaluated (isotropic assumptions) from the measured strains and as calculated using beam theory, on loading with a force in a negative z-direction. Note that σ_1 and σ_2 are not in the material, but in the principal strain direction (I and II).

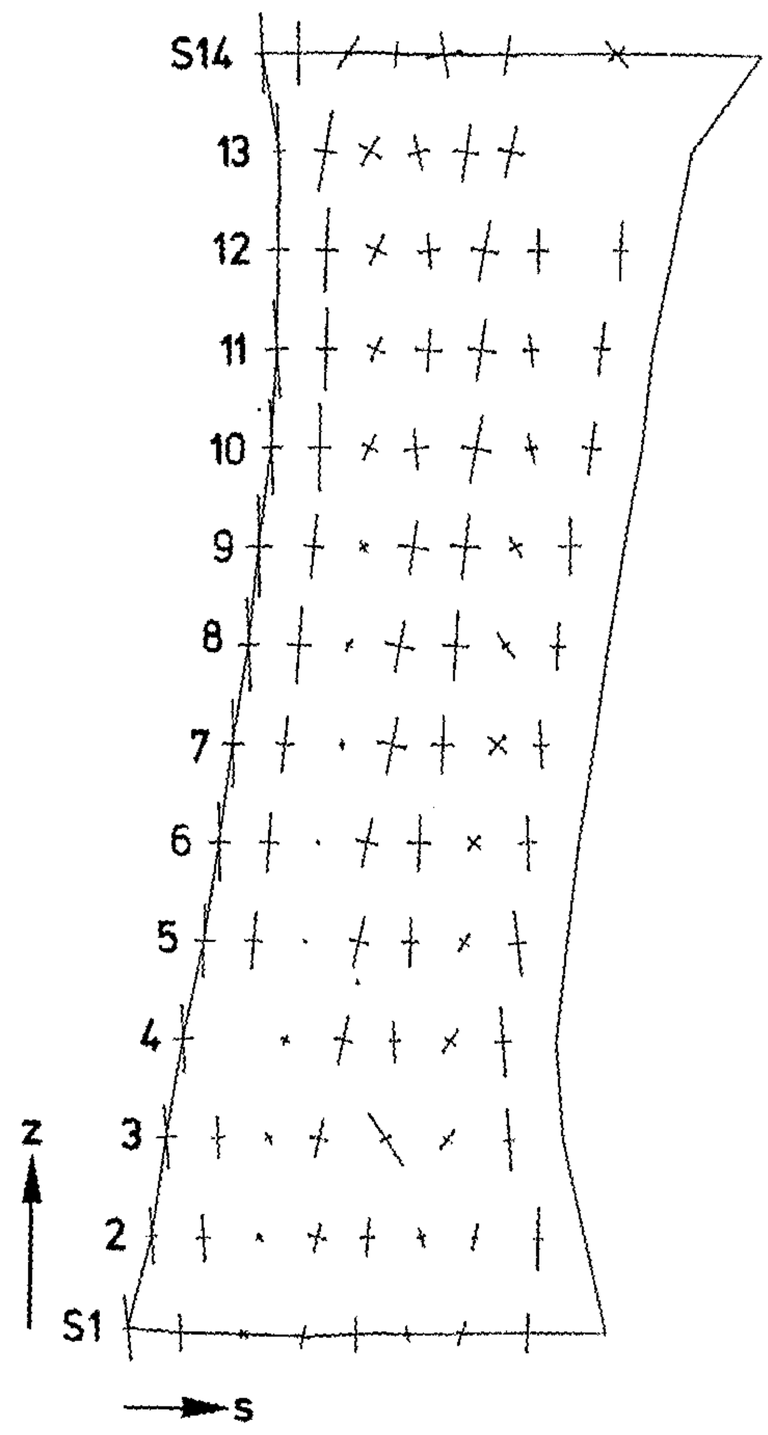

Fig. 10 *Principal strains as measured for a force of 1,000 N in negative z-direction, plotted on the outside femoral surface, developed in a flat plane.*

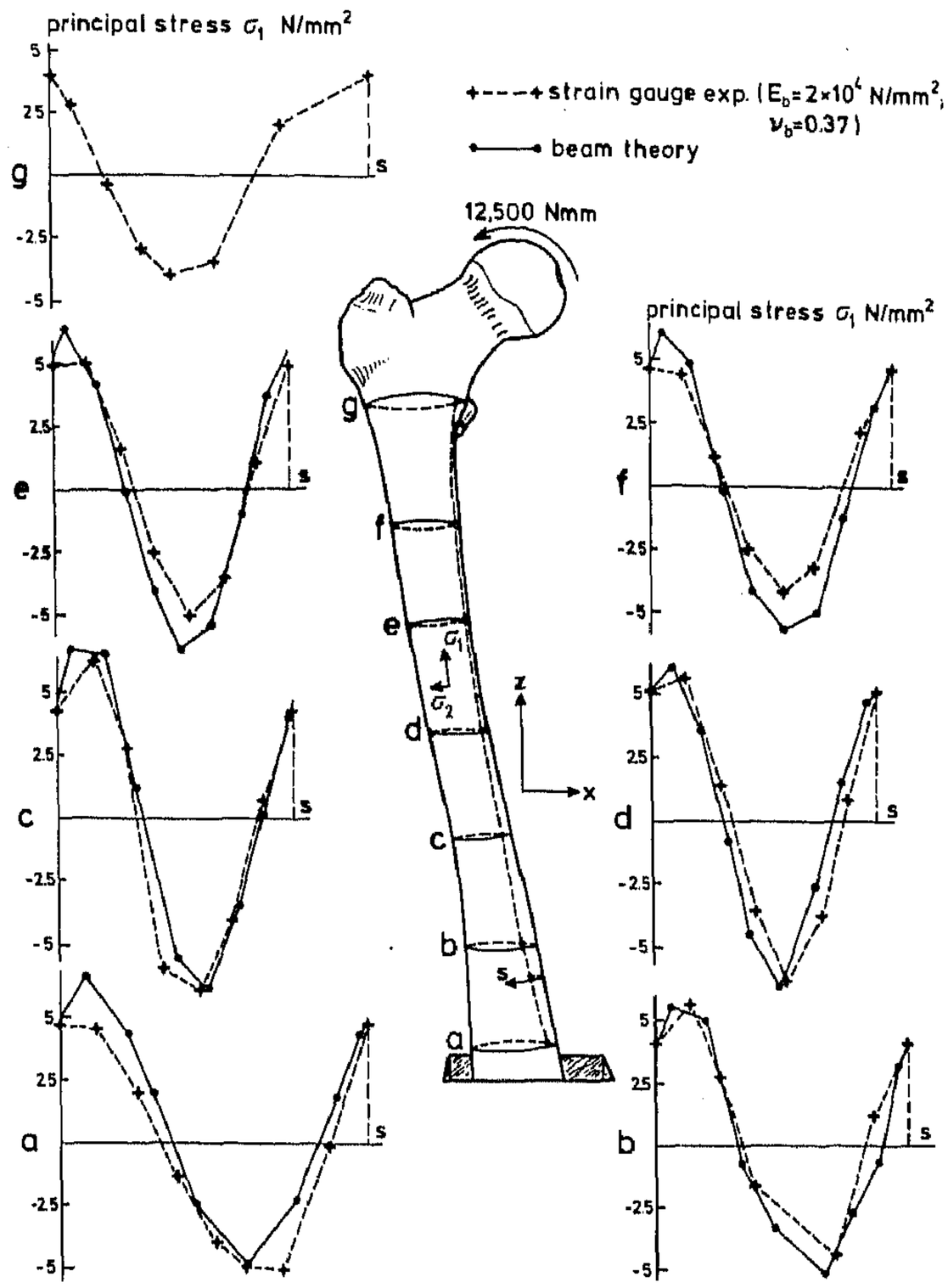

Fig. 11 *Comparison of principal stresses as evaluated (isotropic assumptions) from the measured strains and as calculated using beam theory, on loading with a couple around the y-axis. Note that σ_1 and σ_2 are not in the material, but in the principal strain directions (I and II).*

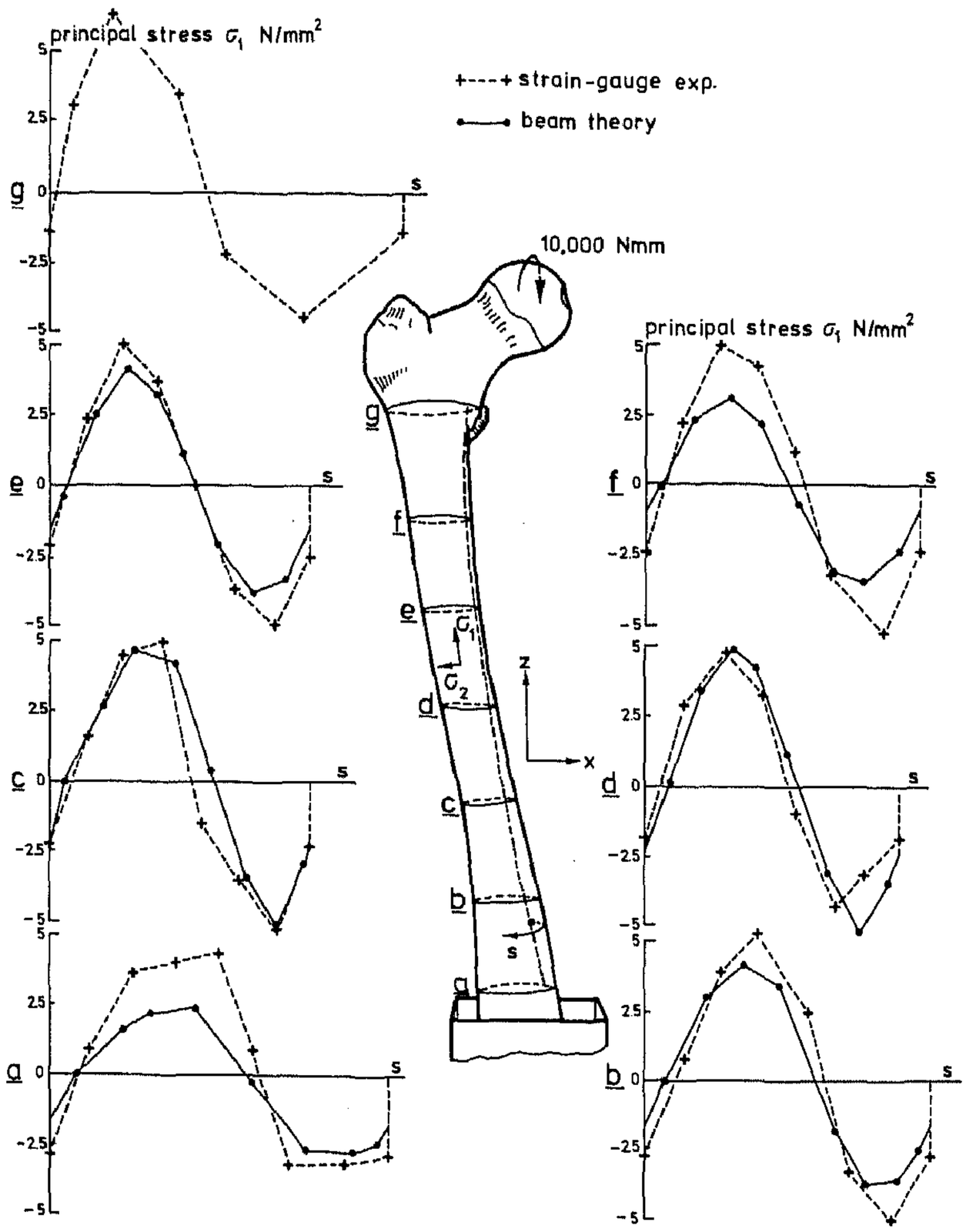

Fig. 12 Comparison of principal stresses as evaluated (isotropic assumptions) from the measured strains and as calculated using beam theory, on loading with a couple around the x-axis. Note that σ_1 and σ_2 are not in the material, but in the principal strain directions (I and II).

Detailed Comparison of Data

For a more elaborate and detailed comparison of data, one section (C12) is chosen. The comparison is more elaborate because also torsion is considered and the axisymmetric model of the section is evaluated as well. It is more detailed because stresses are calculated at the exact strain-gauge locations, no interpolation is carried out, stresses are evaluated in the same local coordinate system, and anisotropy of the bone is considered. Section C12 is shown again in Fig. 13, together with its axisymmetric approximation and the locations of the seven strain gauges (of which No. 41 failed). The angle θ, which defines a bone surface point in the section coordinate system (x',y'), is shown.

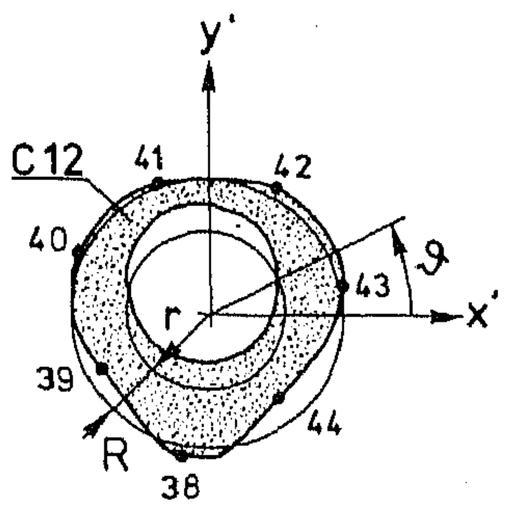

Fig. 13 Section C12 with axisymmetric approximation (R, r). Locations of strain gauges are shown. Angle θ defines a point on the outer bone surface.

Figures 14 and 15 show comparisons of stresses in the principal material coordinate system (σ_1, σ_2 and τ_{12}) for bending moments around the y'-axis (-12,500 Nmm) and the x'-axis (10,000 Nmm) respectively. Experimental results are shown evaluated with both the isotropic and the anisotropic (transversely isotropic) assumptions, and 3-D beam theory results, for the real section geometry as well as for its axisymmetric approximation. Apparently there is only a slight difference between the results of the isotropic and the anisotropic analysis. This is not surprising, since the most significant stress component by far (σ_1) is in the longitudinal direction of the bone, in which the Young's modulus is 20,000 MPa in both cases. Agreement between experimentally obtained and predicted results is excellent in both cases, while the axisymmetric approximation gives quite good results. Since values for σ_2 and τ_{12} are small in the experiment, the principal stress orientation is approximately in the principal material direction.

Section C12 was used for the evaluation of shear stresses upon torsion as well, applying Saint Venant's theory. The result of this analysis is shown in Fig. 16 as maximal shear stresses in the centers of gravity of the 792 elements. As could be expected, the highest shear stresses occur in the narrow part of the cortex. Figure 17 shows a comparison of stresses in the principal material coordinate system (τ_{12}, σ_1, σ_2) upon loading with a torque of 10,000 Nmm. Experimental results are shown, evaluated with both the isotropic and the anisotropic (transversely isotropic) assumptions, the results of the Saint Venant analysis, and the stresses computed for the axisymmetric approximation. In this case, the differences between the isotropic and the anisotropic analyses are substantial. Agreement between experimental shear stresses, evaluated with the anisotropic assumptions, and the Saint Venant predictions is excellent. The direct stress component σ_2, however, which is zero in the Saint Venant analysis, shows a significant value in the experimental results. This may be caused by inaccuracy in the torsional aspect of the applied load, by the geometry of the bone shaft (which is assumed to be prismatic in the Saint Venant analysis) or by local material inhomogeneities.

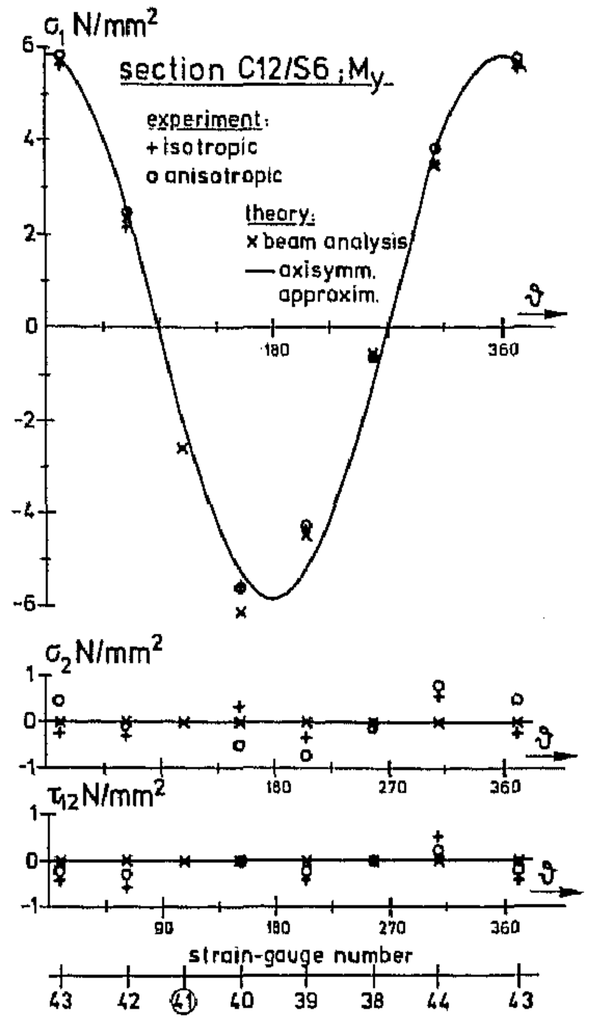

Fig. 14 Comparison of experimental and theoretical stresses in the principal material directions, shown as functions of θ, in section C12, upon loading with a couple $M_y' = -12,500$ Nmm.

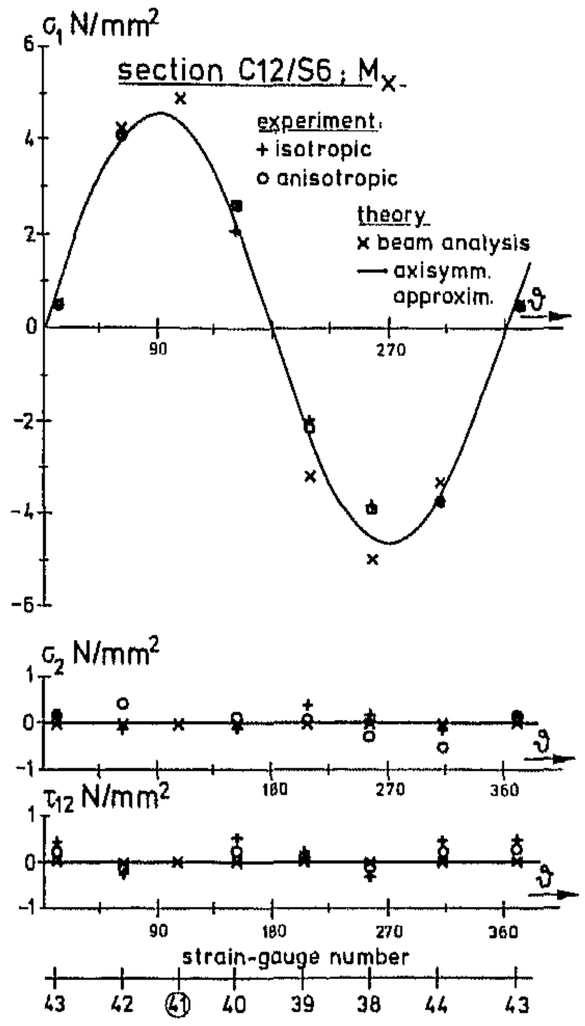

Fig. 15 Comparison of experimental and theoretical stresses in the principal material directions, shown as functions of θ, in section C12, upon loading with a couple $M_x' = 10,000$ Nmm.

Not surprisingly, the accuracy of the axisymmetric approximation is not as good as in the bending case, although the agreement might still be acceptable for some applications.

Saint Venant's analysis was applied to section C12 only. However, evaluations and comparisons for bending stresses and torsional shear stresses using the axisymmetric approximation were carried out for a few other sections as well. The results of these comparisons are comparable to those of section C12 and do not give additional information other than that of consistency in the findings. It is evident that an axisymmetric approximation gives better results

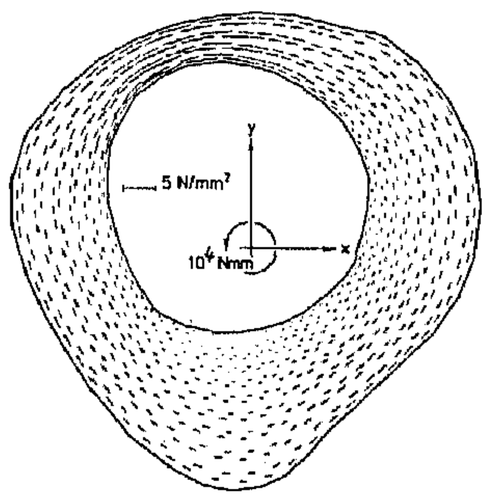

Fig. 16 Maximal shear stresses in section C12 due to torsion, as calculated with the FEM program based on Saint Venant's theory.

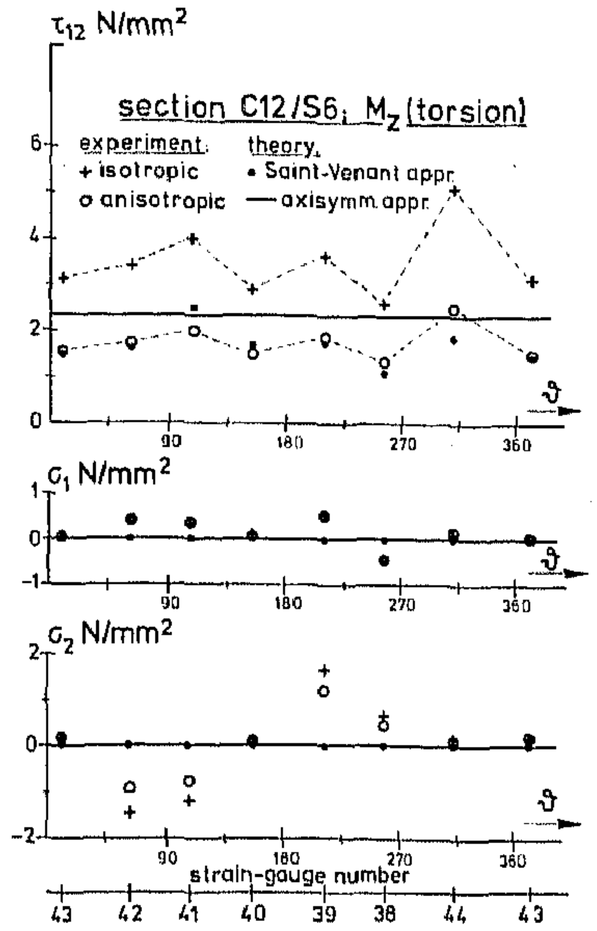

Fig. 17 Comparison of experimental and theoretical stresses in the principal material directions, shown as functions of θ, in section C12, due to loading with a torque M_z = 10,000 Nmm.

when the cross section has a more or less circular countour (Fig. 18), as opposed to a more elliptical shape (Fig. 19), although in the latter case the discrepancies are not dramatic. As an example and for reasons of completeness, Table I shows the values of the principal stress and strain orientation angles with respect to the principal material coordinate system, as calculated from experimental strain values in strain-gauge plane S9 (compare Fig. 3). It is apparent that where stress values are significant, the orientations approximate reasonably well the theoretical predictions (0° for bending, M_x and M_y; 45° for torsion, M_z).

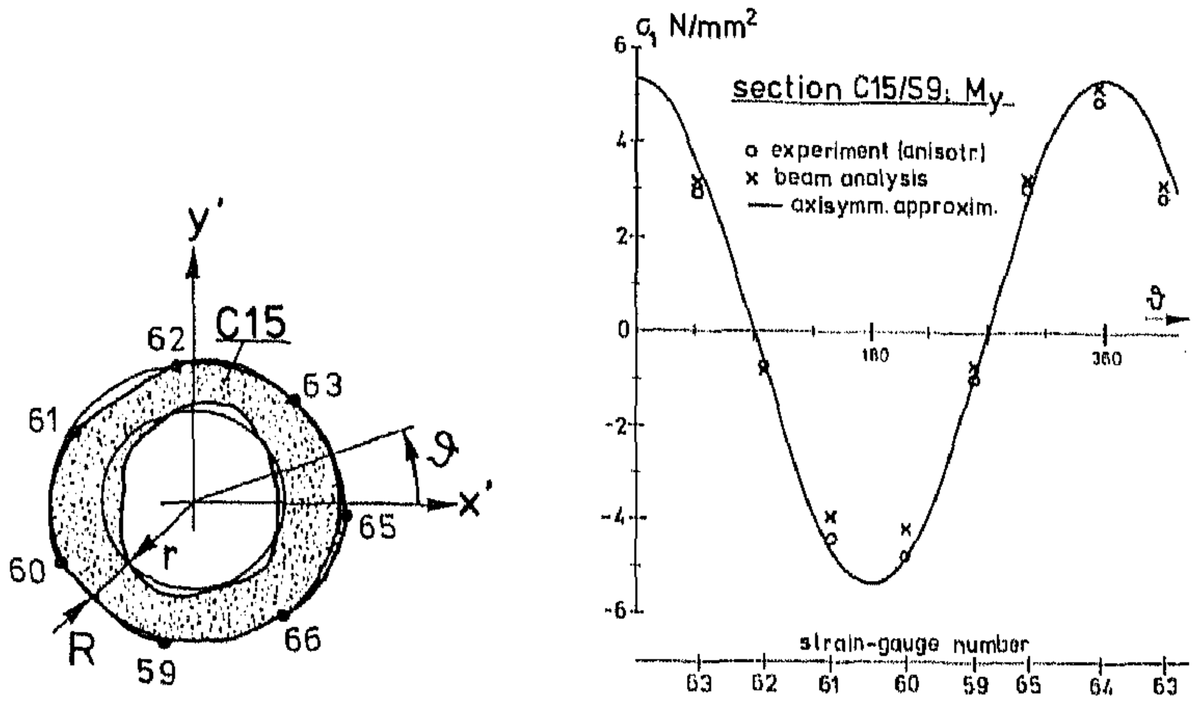

Fig. 18 Comparison of experimental and theoretical values for the stress in the longitudinal bone direction (σ_1) in section C15, due to loading with a couple M_y' = -12,500 Nmm, shown as a function of θ.

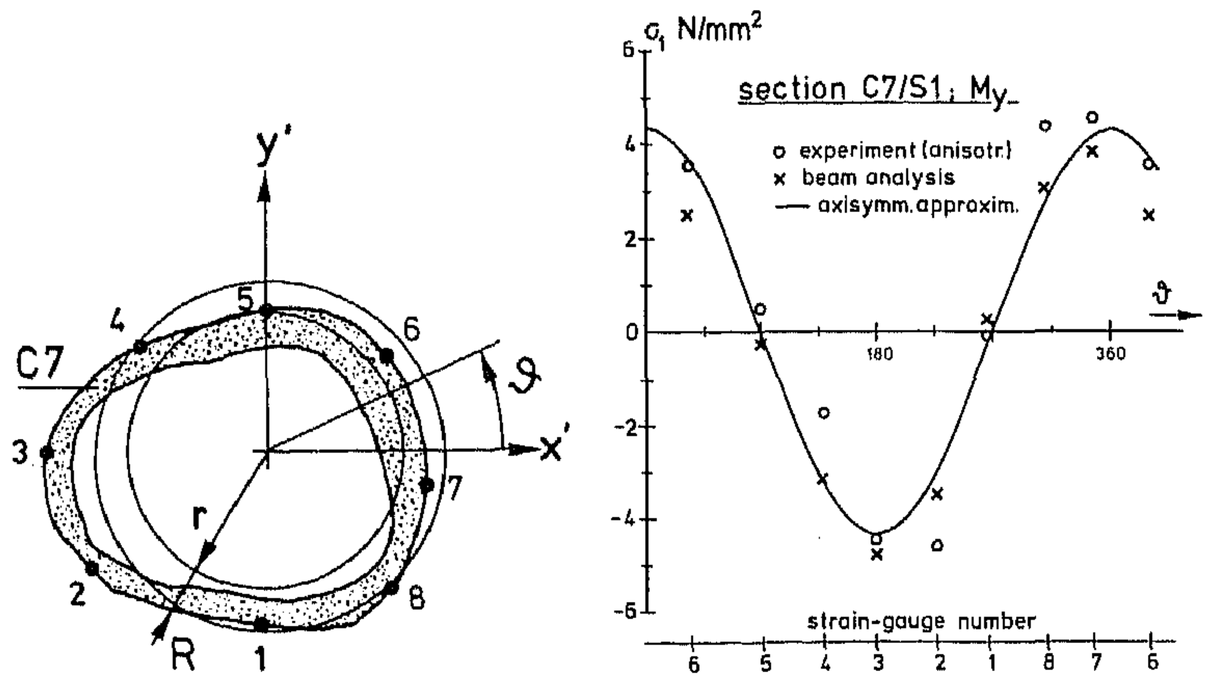

Fig. 19 *Comparison of experimental and theoretical values for the stress in the longitudinal bone direction (σ_1) in section C7, due to loading with a couple $M_y' = -12{,}500$ Nmm, shown as a function of ϑ.*

	M_x		M_y		M_z	
Strain Gauge No.	ϕ	ξ	ϕ	ξ	ϕ	ξ
59	6.5°	3.5°	-8.0°	-4.7°	36°	32.4°
60	-5.4°	-2.9°	3.4°	1.8°	38.5°	35.2°
61	14.0°	7.6°	-1.4°	-0.7°	43.5°	44.1°
62	-5.0°	-2.7°	-31.0°	-22.9°	48.5°	50.9°
63	-8.4°	-4.7°	0.0°	0.0°	54.5°	58.8°
64	0.4°	0.2°	-7.0°	-3.9°	50.0°	51.4°
65	-7.0°	-3.9°	9.3°	5.1°	45.5°	45.9°

Table I *Principal strain (ϕ) and stress (ξ) orientation angles with respect to the principal material axes (Fig. 3), as follow from the transversely isotropic analysis of strains measured for three loading cases.*

Femur with Hip Prostheses

As mentioned previously, the same measurements were carried out for the femur applied with various implants. Only the results for the short- and long-stemmed, cemented Müller prostheses (Fig. 20) will be discussed here. In this case again, strain results for positive and negative couples were essentially equal, indicating linear elastic behavior, and showing also that the prostheses stems were well fixed.

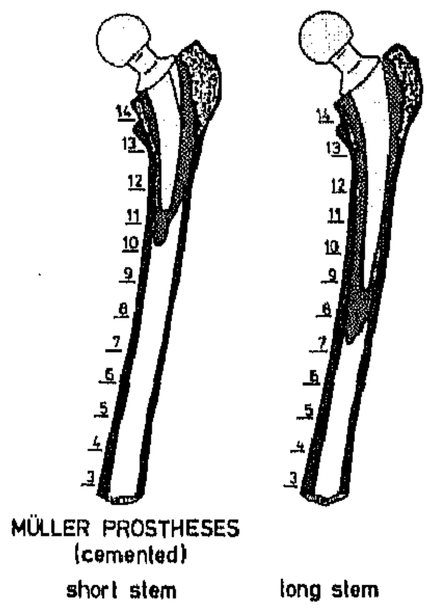

Fig. 20 The two cemented prostheses implanted in the femur.

A comparison between results for the intact femur and the femur with the prostheses is hampered, as far as loading with forces is concerned, by the fact that the positions of the artificial heads were not equal to that of the natural femoral head. Since the bone was loaded with a different loading system, significantly different stress patterns resulted that cannot be related to the influences of the prosthesis stems, a fact that has been neglected to some extent in comparable analyses [e.g. 28]. The effects of pure couple loading do not suffer from this difference in head position and hence, their use is much better suited to investigate the isolated mechanical influences of prosthesis stems, even if this kind of loading is not really physiological.

The results of these measurements do not differ in general from comparable experiments reported in the literature [e.g. 9,10,28,29]. It is thought, however, that the application of pure couples, as discussed above, and the use of significantly more strain gauges as in this case, warrant a more precise quantitative evaluation. Torsion was not applied to the prostheses, which leaves the results of the bending moments M_x and M_y to compare. These gave equivalent results, qualitatively speaking, so that only those for the bending moment M_y (principal stresses evaluated using the isotropic assumptions) are shown in Fig. 21. As should be the case, the stress values below the stem tips are in essence equal. On the proximal side, the stems take over a part of the total load that would otherwise be fully carried by the bone, which results in lower bone stresses in the treated femur. This is known as "stress-shielding." It is evident from Fig. 21 that this stress-shielding effect plays an important role on the proximal side only. All stress curves on each level follow a more or less sinusoidal course, indicating that the bone with prosthesis still behaves according to beam theory by good approximation. The principal strain orientations hardly change as a result of the prostheses, as is shown in Fig. 22. Only on the proximal side are some minor deviations seen. It is evident that, apart from the stress-shielding effect, the stresses on the outside femur are rather insensitive to the prosthesis stems.

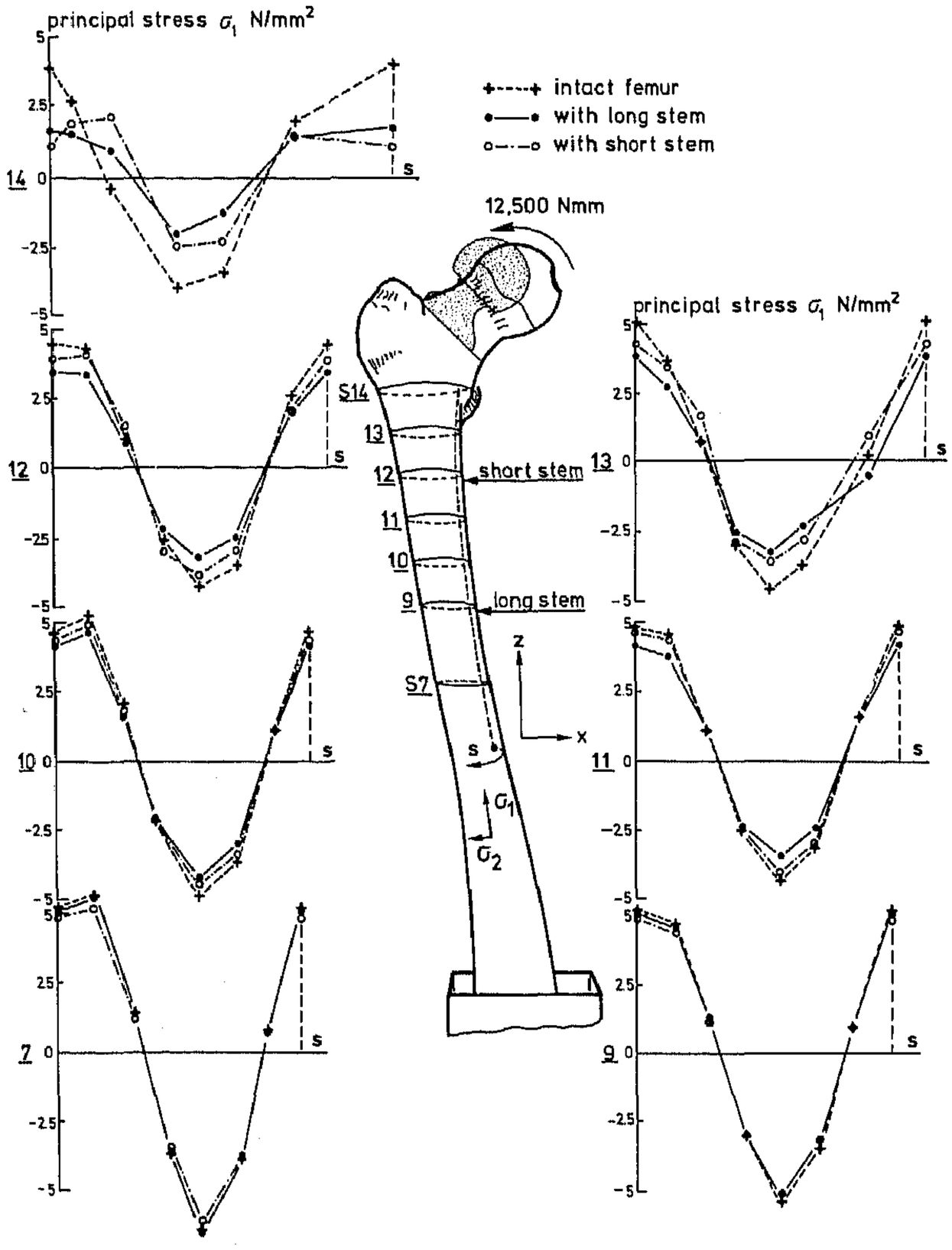

Fig. 21 *Comparison of principal stresses as evaluated (isotropic assumptions) from the measured strains due to loading with a couple around the y-axis, for the intact femur and after implantation of the prostheses. Note that σ_1 and σ_2 are not in the material, but in the principal strain directions (I and II).*

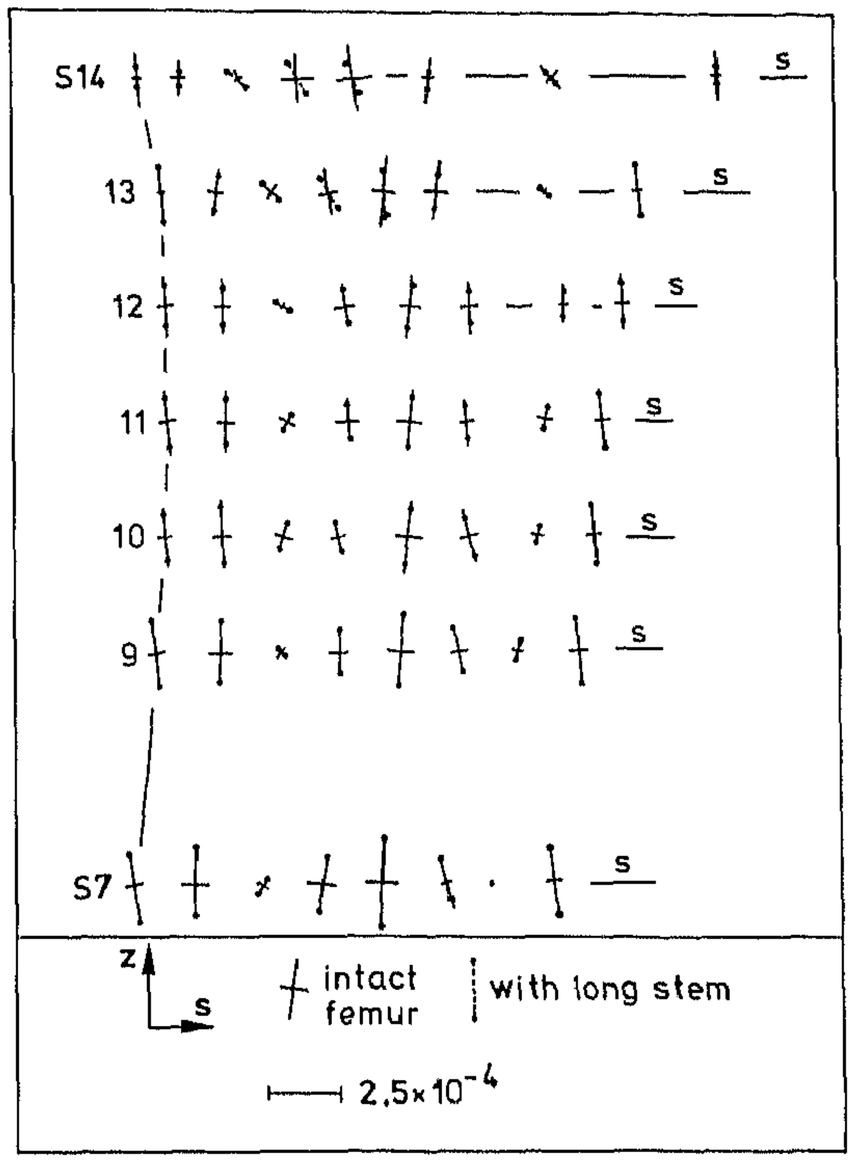

Fig. 22 Principal strains on the same levels as those in Fig. 21, for the same loading, comparing results for the femur with and without long Müller prostheses.

DISCUSSION

It should be kept in mind when interpreting the results presented here, that the experimental femur was embalmed in formaline. This was necessary in order to allow for the bone to retain consistent properties throughout the testing period. Also, embalming keeps the bone from drying out, especially locally due to the strain-gauge heat, which would cause considerable drift in the measured strain values. It is probable, however, that the material properties of this embalmed bone differ from those of a fresh one. Evans [30] has found that embalming human cortical bone increases its Young's modulus in the longitudinal bone direction by around 12%.

It was assumed in the comparisons between experimental and theoretical data, that the geometries of the left and the right femurs were images of one another. Although an overall dimensional comparison of both bones did not show any significant differences, no detailed evaluation was carried out. Another possible source of error lies in the interpolation procedure necessary in the overall comparison of measured and predicted data. However, owing to the relatively gradual change in diaphysis geometry, it is thought that these errors are small. It is clear, of course, that both the strain measurements and the determination of cross-sectional properties are subject to random errors.

In applying beam theory, the stresses calculated are independent of the elastic properties of the bone. Hence, the agreement found between measured and calculated values reflects a good choice for the Young's modulus, although 20,000 MPa is somewhat higher than usually mentioned as average for cortical bone [e.g. 22,30]. However, this could easily be a result of the embalming procedure. In any case, a better overall fit of the curves cannot be obtained by adjusting this value.

The shear stresses calculated with Saint Venant's theory for torsion, too, are independent of the shear modulus. Hence, the agreement between measured (anisotropically evaluated) and predicted data found here again reflects the good choice of the longitudinal Young's modulus, and lends confidence to the applicability of the transversely isotropic elastic constants determined by Reilly and Burstein [21,22].

Carter [21] concluded that by evaluating strain data from cortical bone, using anisotropic (transversely isotropic) assumptions, significantly different results are found as compared to isotropic assumptions. This was not confirmed here with respect to the most significant stress components in bending and axial loading. This discrepancy is obviously caused by the fact that these stress components are in the longitudinal material direction, and because it was assumed here that the Young's moduli in this direction are equal in both the isotropic and anisotropic cases. Carter [21], on the other hand, chose an average of longitudinal and transverse moduli for his isotropic analysis, which is rather unrealistic for this type of loading. His conclusions are correct, however, if other stress components in the above-mentioned loading cases are concerned, and if torsion is applied.

It is evident from the results presented here that when the cortical bone is assumed to behave linear elastic, homogeneous and transversely isotropic, and when the bone geometry is represented correctly, a quite accurate prediction of stress patterns in the bone under arbitrary loading should be possible by using FEM. Some local inaccuracies, however, should be expected as a result of local inhomogeneities in bone stiffness as well as some geometrically nonlinearities on loading with an axial force. Even when the cortical bone is assumed to be completely isotropic, a good theoretical prediction of the most significant stresses on bending and axial loading should be possible. This contradicts the conclusions expressed by Rohlmann et al. [10]. It is possible that the discrepancies between strain gauge and FEM results reported by them are due principally to an inadequate mesh refinement, almost unavoidable in a three-dimensional FEM analysis as yet, in view of the computer costs. Evidently, three-dimensional beam theory gives much better possibilities for approximate stress analysis of structures of this kind.

When requirements of accuracy are not too high, and when only the most significant components are of interest, the bone shaft can be represented by an axisymmetric model for all loading cases. The properties of such a model, valid for the bone analyzed here, are tabulated in Table II. Although the values of I_{appr}, the area moment of inertia of the axisymmetric approximation, increases significantly at the proximal and distal ends, the area moment of resistance W_{appr} ($= I_{appr}/R$) shows a much more homogeneous behavior, as does the cross-sectional area A. The same is true for the area moments of resistance, W_{max} and W_{min}, of the real sections (Table II). Since the areas and moments of resistance determine the maximal stresses on the bone surface on axial loading and bending, this explains why these maximal stresses do not change very much from proximal to distal (Figs. 11 and 12). It also indicates that the bone diaphysis might have been structured in such a way as to have homogeneous structural strength. In view of the data in Table II, it would certainly be acceptable in approximate stress analyses to represent a part of the diaphysis by a cylinder of homogeneous cross section.

The results obtained for the femur provided with hip endoprostheses indicate that in this case too, the femur behaves according to linear beam theory, although at the proximal side some disturbance is apparent. These tendencies can also be recognized in the results of Jacob et al [9]. Stress-shielding effects, which are thought to be responsible for bone resorption and disuse osteoporosis, are of significance at the outermost proximal side only. It should be recognized that the higher the axial direct stresses in the proximal bone, the less stress shielding will occur; however, more shear and direct stress will be exerted at the proximal side in the cement mantle and at the inner cortical surface [31], which can result in cement fracture, and could be responsible for bone resorption as well.

Section	R(mm)	r(mm)	$I_{appr}(mm^4)$	$W_{appr}(mm^3)$	$A(mm^2)$	$W_{max}(mm^3)$	$W_{min}(mm^3)$
C6	21.2	18.1	7.5	0.35	3.8	3.4	1.8
C7	18.9	16.4	5.4	0.29	3.8	3.0	1.9
C8	16.6	13.0	3.7	0.22	3.3	2.3	2.0
C9	16.6	13.0	3.7	0.22	3.3	2.3	2.0
C10	15.6	10.6	3.6	0.23	4.1	2.4	2.2
C11	14.7	9.4	3.1	0.21	4.0	2.1	1.8
C12	14.6	8.7	3.1	0.21	4.3	2.3	1.7
C13	15.1	9.7	3.4	0.23	4.2	2.7	1.8
C14	14.8	8.6	3.3	0.22	4.5	2.2	2.0
C15	15.2	9.5	3.5	0.23	4.4	2.4	2.1
C16	15.1	9.3	3.5	0.23	4.5	2.5	1.9
C17	16.1	11.2	4.0	0.25	4.2	2.7	1.8
C18	16.3	11.4	4.2	0.26	4.3	2.8	2.0
C19	18.1	13.6	5.7	0.31	4.4	3.6	2.3
C20	21.4	17.6	9.0	0.42	4.7	4.5	2.7

Table II Values for the outer (R) and inner (r) radii of the axisymmetric approximations for each section, their area moments of inertia (I_{appr}), area moments of resistance (W_{appr}) and areas (A). Also showing maximal and minimal area moments of resistance (W_{max} with respect to I_{max}, W_{min} with respect to I_{min}) of the real sections.

It is obvious that femoral surface stress patterns do not provide accurate information about stresses in the prosthesis stems, the cement mantle, or at the stem-cement and cement-bone interfaces. Hence, in order to more closely investigate the load transmitting mechanism and evaluate the mechanical influences of the stem, theoretical stress analyses have to be applied. Several studies of this kind, mostly using FEM, were reported in the recent literature (for an extensive review see [31]). Although the FEM is very well suited to analyze irregular structures of this kind in principle, its application does have two disadvantages. The first of these is a temporary one. In view of computer expenses and requirements of data handling, it is presently quite difficult to apply an adequately refined three-dimensional element mesh for this bone-prosthesis structure. Moreover, certain aspects of this structure, as for example the behavior of the stem-cement and cement-bone interfaces, have not been investigated to a point where they can be accurately accounted for in a refined three-dimensional model. No doubt these problems will be solved in the course of time, when faster computers and more sophisticated programs become available, and when more research has been done. The second disadvantage, however, is a principle one. A three-dimensional FE model of such a bone-prosthesis structure is always quite specific, which makes it hard to derive general principles from its results. Because of the complexity of the model, and due to the fact that in a numerical solution procedure the number of parametric variations that can be investigated is finite, it is nearly impossible to establish a clear concept of the relations between structural properties and stress patterns. This, of course, is not so much a problem when specific questions have to be answered concerning, for example the effects of certain

design alternatives, or the evaluation of one specific design relative to another. However, it is a disadvantage when general design and fixation guidelines are required.

Based on the results presented in this paper, and in view of FEM results [10] previously discussed here, the conclusion is justified that when comparing the complexity, computer costs and the potential accuracy of FE models to three-dimensional beam models, the latter have some advantages when used to analyze the femoral diaphysis. Since it is suggested by the results presented here that the femur with prosthesis, too, behaves in a beam-like manner, a more simple and direct approach to the analysis of these structures can be taken. For, the prosthesis stem, no doubt, behaves as a beam, and when the bone does too, the structure can simply be modeled as two beams continuously connected by an elastic intermediate, the cement mantle. Such a structure can be represented by a FE beam model [31], in which the stem and the bone are described by beam elements and the cement mantle by more sophisticated three-dimensional elements. Moveover, when the model is geometrically simplified to homogeneous cross sections, beams-on-elastic-foundation theory can be applied [31] which results in closed-form solutions, giving formulas that relate the most important structural parameters directly to the most significant stresses in all three materials and at their interfaces. Of course, especially in the latter case, only approximate results can be expected. However, these methods are extremely helpful in developing rough but simple analytic design and fixation guidelines [31,32] that could never be obtained from complex three-dimensional FE models. Also, these methods can be used to better understand the results of complex models, put them in a more general setting, and execute the necessary parametric analyses that would be too costly for an accurate three-dimensional FE model. The latter would then be used more as a reference model than as a direct research tool.

CONCLUSION

Based on the results presented here, it can be concluded that the human femur, at least the extended femoral shaft, behaves as a linear elastic, homogeneous and transversely isotropic beam. However, geometrically nonlinear behavior results when it is loaded with axial forces, while local impurities in stiffness properties occur. Values for transversely isotropic elastic constants of cortical bone as published in the literature [21,22], appear adequate to characterize this material in structural stress analyses.

When only the most significant stress components are of interest, and no torsion is considered, the cortical bone material can, with good approximation, be assumed as isotropic. A less accurate but still reasonable approximation results when the bone is modeled as an axisymmetric structure in such a way that cross-sectional areas and polar moments of inertia are reproduced.

When hip endoprostheses are inserted inside the medullary canal, the stress patterns on the outside surface of the bone on loading can give no accurate indications of stress distributions within the structure, although the stress-shielding effect is apparent. The bone still behaves in a beam-like manner.

ACKNOWLEDGEMENTS

The data on which the present results are based were obtained from a number of research projects, involving several students, technicians and scientists of the Div. of Applied Mechanics, Eindhoven University of Technology. Especially W. A. Brekelmans, F.v.d. Broek, P. C. v. Heugten, W. Laaper, F. E. Veldpaus and J. IJzermans have contributed to these efforts.

We are indebted to J. E. Bechtold and H. S. Shyr (Biomechanics Lab, Mayo Clinic) for their contributions to measurements and computations in the final stages of this work, and to T. E. Crippen for his elaborate review of the manuscript and useful suggestions.

Finally, we wish to acknowledge a grant from The Netherlands Organization for the Advancement of Pure Research (ZWO), by which the principal author is presently supported.

REFERENCES

1 Evans, F.G., "Stress and Strain in Bones," Charles C. Thomas, Springfield, IL, 1957.

2 Küntscher, G., "Die Darstellung des Kraftflusses im Knochen," Zentralbl. Chir., Vol. 61, 1934, pp. 2130-2136.

3 Brockhurst, P.J., and Svensson, N.L., "Design of Total Hip Prosthesis," Med. Progr. Technol., Vol. 5, 1977, pp. 73-102.

4 Hallermann, E., "Die Beziehungen der Werkstoffmechanic und Werkstoff-forschung zur algemeinen Knochen-Mechanik," Verhandl. Deutsch. Orthop. Gesellsch., Vol. 62, 1934, pp. 347-360.

5 Pauwels, F., "Ueber die Bedeutung der Bauprinzipien des Stütz-und Bewegungsapparates für die Beanspruchung der Röhrenknochen," Acta Anat., Vol. 12, 1951, pp. 207-227.

6 Küntscher, G., "Die Spannungsverteilung am Schenkelhals," Arch. Klin. Chir., Vol. 185, 1936, pp. 308-321.

7 Slooff, T.J., "Spannungsveränderungen im proximalen Femurende bei einzementierten Endoprosthesen," Arch. Orthop. Unfall-Chir., Vol. 71, 1971, pp. 281-289.

8 Huiskes, R., Heugten, P.C.M.v., and Slooff, T.J., "Strain-Gauge Measurements on a Loaded Femur, Intact as well as Provided with Prostheses," Proceedings of the 29th ACEMB, Boston, MA, November, 1976.

9 Jacob, H.A.C., and Huggler, A.H., "An Investigation into Biomechanical Causes of Prosthesis Stem Loosening within the Proximal End of the Human Femur," J. Biomech., Vol. 13, 1980, pp. 159-173.

10 Rohlmann, A., Bergmann, G., and Kölbel, R., "The Relevance of Stress Computation in the Femur with and without Endoprostheses," Int. Conf. Proceedings, Finite Elements in Biomechanics, (B.R. Simon, Ed.), The Univ. of Arizona, Tucson, Vol. 2, 1980, pp. 549-567.

11 Meyer, H., "Die Architectur der Spongiosa," Archiv. f. Anat. Phys. u. Wissensch. Medizin, 1867, P. 615.

12 Koch, J.C., "The Laws of Bone Architecture," Am. J. Anat., Vol. 21, 1917, pp. 177-298.

13 Toridis, Th.G., "Stress Analysis of the Femur," J. Biomech., Vol. 2, 1969, pp. 163-174.

14 Rybicki, E.F., Simonen, F.A., and Weis, E.B., "On the Mathematical Analysis of Stress in the Human Femur," J. Biomech., Vol. 5, 1972, pp. 203-215.

15 Scholten, R., "Ueber die Berechnung der mechanische Beanspruchung in Knochenstrukturen mittels für den flugzeugbau entwickelte Rechenverfahren," Med. Orthop. Technik, Vol. 6, 1975, pp. 130-138.

16 Brekelmans, W.A.M., Poort, H.W., and Slooff, T.J., "A New Method to Analyse the Mechanical Behavior of Skeletal Parts," Acta Orthop. Scand., Vol. 43, 1972, pp. 301-317.

17 Wood, R.D., Valliappan, S., and Svensson, N.L., "Stress Analysis of Human Femur," Theory and Practice in FEM Structural Analysis, (Y. Yamada and R.H. Gallagher, Eds.), Univ. of Tokyo Press, Tokyo, Japan, 1973.

18 Olofsson, H., "Three-Dimensional FEM Calculation of Elastic Stress Fields in Human Femur," Thesis, Inst. of Technology, Uppsala, Sweden, 1976.

19 Valliappan, S., Svensson, N.L., and Wood, R.D., "Three-Dimensional Stress Analysis of the Human Femur," Comput. Biol. Med., Vol. 7, 1977, pp. 253-264.

20 Valliappan, S., Kjellberg, S., and Svensson, N.L., "Finite Element Analysis of Total Hip Prosthesis," Int. Conf. Proceedings, Finite Elements in Biomechanics, (B.R. Simon, Ed.), The Univ. of Arizona, Tucson, Vol. 2, 1980, pp. 549-567.

21 Carter, D.R., "Anisotropic Analysis of Strain Rosette Information from Cortical Bone," J. Biomech., Vol. 11, 1978, pp. 199-202.

22 Reilly, D.T., and Burstein, A.H., "The Elastic and Ultimate Properties of Compact Bone Tissue," J. Biomech., Vol. 8, 1975, pp. 393-405.

23 Timoshenko, S.P., and Goodier, J.M., "Theory of Elasticity," 3rd ed., McGraw-Hill, Kogahusha, Tokyo, Japan, 1970.

24 Brekelmans, W.A.M., "A FEM Program for the Numerical Solution of a Certain Kind of Elliptical Differential Equations," (in Dutch), Rpt. No. WE-75-03, Div. Appl. Mech., Mech. Eng., Eindhoven Univ. of Technology, The Netherlands, 1975.

25 Piotrowski, G., and Wilcox, G.A., "The Stress Program: A Computer Program for the Analysis of Stresses in Long Bones," J. Biomech., Vol. 4, 1971, pp. 497-506.

26 Piziali, R.L., Hight, T.K., and Nagel, D.A., "An Extended Structural Analysis of Long Bones, Application to the Human Tibia," J. Biomech., Vol. 9, 1976, pp. 695-701.

27 Carter, D.R., Vasu, R., Spengler, D.M., and Dueland, R.T., "Stress Fields in the Unplated and Plated Canine Femur Calculated from in vivo Strain Measurements," J. Biomech., Vol. 14, 1981, pp. 63-70.

28 Oh, I., and Harris, W.H., "Proximal Strain Distribution in the Loaded Femur," J. Bone Joint Surg., Vol. 60-A, 1978, pp. 75-85.

29 Crowninshield, R.D., Pedersen, D.R., and Brand, R.A., "A Measurement of Proximal Femur Strain with Total Hip Arthroplasty," J. Biomech. Eng., Vol. 102, 1980, pp. 230-233.

30 Evans, F.G., "Mechanical Properties of Bone," Charles C. Thomas, Publ., Springfield, IL, 1973.

31 Huiskes, R., "Some Fundamental Aspects of Human Joint Replacement," Acta Orthop. Scand., Supplement No. 185, 1979, pp. 109-199.

32 Huiskes, R., Crippen, T.E., Bechtold, J.E., and Chao, E.Y., "Analytic Guidelines for Optimal Stem Designs of Custom-Made Joint Prostheses," submitted 1981.